

QUILL

Quarterly Reports



November 2020 – January 2021



All information held within is confidential and is

Copyright © QUILL 2021.

It contains proprietary information which is disclosed for information purposes only.

The contents shall not in whole or in part

(i) be used for other purposes,

(ii) be disclosed to any person not being a member of staff or student of QUILL

(3 year period up to February 2024)

(iii) be disclosed to any person not being a member of staff of a QUILL industry member or one of their affiliated companies,

(iv) be stored in any retrieval system, or reproduced in any manner which does not fulfil conditions (i), (ii) and (iii) without the written permission of the Director of QUILL, The Queen's University of Belfast, David Keir Building, Stranmillis Road, Belfast BT9 5AG, United Kingdom.

Contents

Valorisation of Products from Waste Plastic Pyrolysis (Issam Abdalghani)	4
Design of New, Non-coordinating, and Hydrophobic Anions for Functional Ionic Liquids (Haris Amir)	5
Lithium Ion Batteries Degradation Study Using Spectroscopy Techniques (Marian Borucki)	8
Recycle and Reuse of Process Water Through Sulfate Removal: Developing an Ionic Liquid Technology for Selective Anion Recognition and Extraction (Dominic Burns)	12
Battery Thermal Management and Algorithmic 3D Temperature Prediction (Andrew Forde)	13
Mechanism Understanding of NO _x storage, release and reduction on Pt/doped ceria catalysts (Oisin Hamill)	15
A Catalytic Gas-to-Liquid Process for CO Valorisation (Jerry Li)	17
Chemisorbent Materials for Olefin and Paraffin Separation (Sam McCalmont)	20
Boron Lewis Acids: Structure and Applications (Anne McGrogan)	22
Thinking Inside the (Glove)Box: Lewis Superacidic Ionic Liquids Based on Main Group Cations (Shannon McLaughlin)	27
Redox Flow Battery Design (Hugh O'Connor)	32
Developing New Nanocatalysts for the Direct Conversion of Biogenic Carbon Dioxide (CO ₂) to Sustainable Fuels (Zara Shiels)	33
Thermochemical Conversion of Biomass Lignin into Mesoporous Carbon Materials (Yaoguang Song)	35
Modelling the use of Flow Batteries in Transport Applications (Richard Woodfield)	40
Gas Separation Technologies (Mark Young)	41

QUILL Quarterly Report

November 2020 – January 2021

Name:	Issam Abdalghani		
Supervisor(s):	Gosia Swadźba-Kwaśny		
Position:	Post-doctoral Researcher		
Start date:	10/12/2019	Anticipated end date:	08/03/2021
Funding body:	Invest Northern Ireland (Proof of Concept Funding Scheme)		

Valorisation of Products from Waste Plastic Pyrolysis

During this period, I have more focused on the study of the effect of heteroatoms present in the feedstock on the reactivity of the Lewis acidic ionic liquids (Liquid coordination complexes (LCCs, chloroaluminate ionic liquids and borenium ionic liquids). I have pre-treated naphtha (C₅-C₁₂) feedstock with silica in order to reduce the concentration of the heteroatoms, while analysed them using XRF before and after treatment (**Table 1**).

Table 1 - The XRF analysis of both real and pre-treated naphtha.

No.	Component	Real naphtha (ppm)	Pre-treated naphtha (ppm)
1	Si	170	86.3
2	S	163	116
3	Cl	105	59.5
4	Al	ND	ND
5	P	ND	80.5

Furthermore, I screened the oligomerization of the feedstock using Lewis acidic ionic liquids to compare the results with the case of real feedstock. As a result, In the case of borenium ionic liquids which showed the best results, I found that the activity of the catalysts using the pre-treated feedstock was higher than in the case of using real feedstock. On the other hand, the product distribution (C₂₀-C₅₀ oligomers) was different as shown in **Table 2**. Currently, I am working on the analysis of the physical properties of the products (KV and VI).

Table 2 - Simulated Distillation-GC results and product distribution using borenium ionic liquids.

Catalyst loading (wt%)	oligomer fraction distribution				Total C ₂₀₊
	C ₂₀ -C ₃₀	C ₃₀ -C ₄₀	C ₄₀ -C ₅₀	C ₅₀₊	
5	8	5	3	2.5	18.5
10	18	14	8	7.5	47.5
20 ^a	19	16	15	6.5	56.5
20 ^b	18	20	17	21.5	76.5
20 ^c	18	21	17	20.5	76.5

^aOligomerization conditions: 10 g naphtha (without purification), [BCl₂(L)] [Al₂Cl₇](L= 4-picoline) (5-20 wt%), 25 °C, 600 rpm, 20 h.

^bUsing [BCl₂(L)] [Al₂Cl₇](L= 4-picoline), and pre-treated naphtha.

^c using [BCl₂(L)] [Al₂Cl₇](L= 3-picoline), and pre-treated naphtha.

QUILL Quarterly Report

November 2020 – January 2021

Name:	Haris Amir		
Supervisor(s):	Prof John Holbrey		
Position:	Postgraduate (PhD)		
Start date:	01/10/2020	Anticipated end date:	30/09/2023
Funding body:	ESPRC/UKRI		

Design of New, Non-coordinating, and Hydrophobic Anions for Functional Ionic Liquids

These studies focus on the generation and investigation of new boron-based anions that can be applied to formation of ionic liquids. A series of O- and N-chelated borate anions and mixed alkoxy/cyanoborate anions are under investigation.

Borate Ester Anions:

Following on from the initial strategy the synthesis of different borate ester anions was investigated. The initial approach used was to form an alkali borate ester salt, however this was subsequently changed to target formation of the borate anions with a free proton. The reason behind this change was firstly to determine whether the free proton was observable using ^1H NMR spectroscopy and secondly to measure the Lewis acidity of the proton using trioctylphosphine oxide (TOPO) as a spectroscopic probe, calculating the difference in chemical shift in the ^{31}P NMR spectra. Deviations of borate ester anions were attempted such as with diamine and amino butanol. In some cases, using triols to synthesise borate ester anions, the remaining pendant hydroxy group was then reacted with long chain carboxylic acids in an esterification reaction. This was done to determine how ester functional groups can affect the physical and chemical property of the anion.

The first attempt at forming borate esters was performed following a published route. The reaction scheme is shown in figure 1.

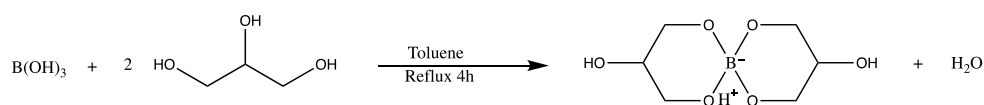


Figure 1 - Reaction scheme for the formation of glycerol borate ester anions.¹

This reaction was straightforward with a yield of 66%, the free proton as seen in figure 1 was not detected in the ^1H NMR, making the Lewis acidity of the proton difficult to determine. Glycerol is a triol giving a hydroxy group on either side as depicted in figure 1, and has been reported to coordinate to boron through the terminal hydroxyl sites allowing the central hydroxy group to be derivatised by reaction with long chain carboxylic acids via esterification. This has been attempted with two different carboxylic acids (lauric acid and stearic acid). A general synthetic route of this reaction is shown in figure 2.

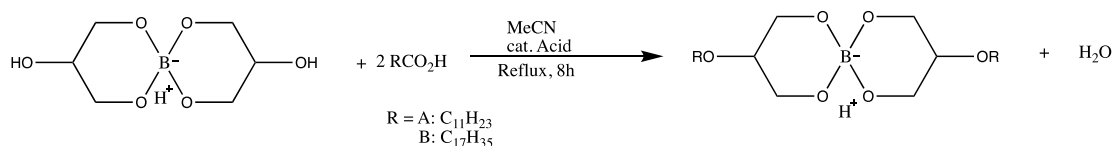


Figure 2 - Esterification of glycerol borate ester anions.

Both attempts produced very low yield (27%) of the desired product which was obtained as a waxy solid when lauric acid was used and as a white powder when stearic acid was used. This suggests that short chained carboxylic acids should be used instead in order to obtain proton acidic ionic liquids.

The other derivatives of this anion are shown in figure 3, in all cases the desired product was obtained in high yields (>65%). The formation of nitrogen–boron bonds reduced the viscosity of the product dramatically when compared to being bonded to oxygen alone. This leads to the idea if boron was bonded to only nitrogen the viscosity of the anion would be trivial and at room temperature would be completely a liquid.

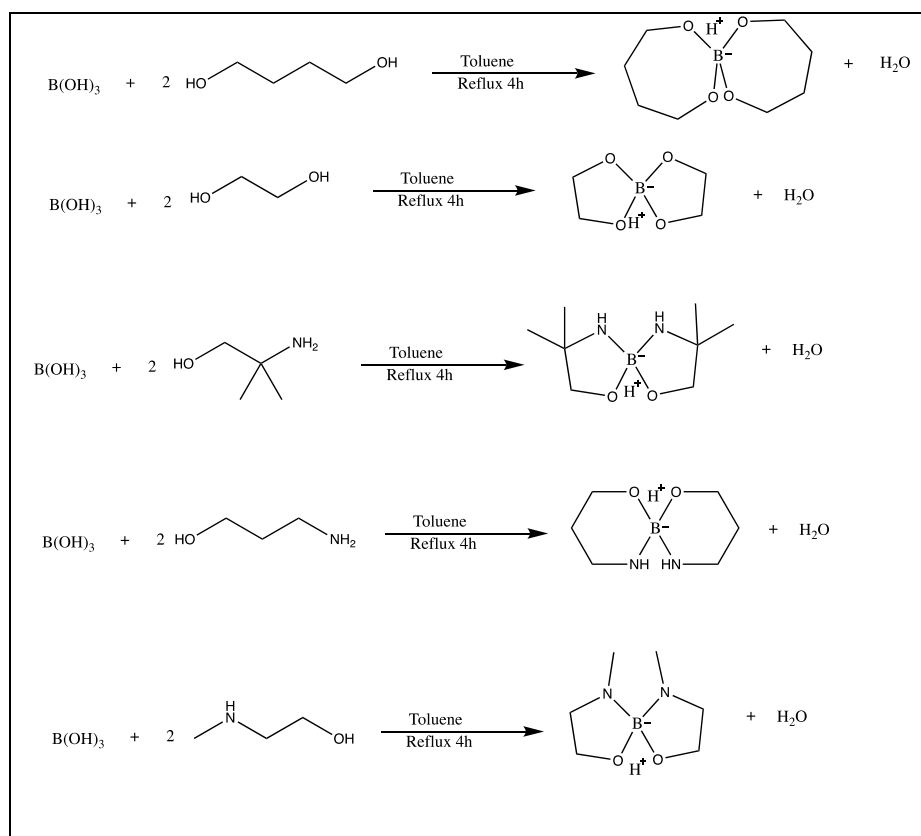


Figure 3 - The synthesis of borate ester anion derivatives.

Future work with borate ester derivatives would be to react with diamines and investigate how that will influence the functionality of the borate anion.

Tetraalkoxyborate Anions:

The synthesis of sodium tetraalkoxyborate $\text{Na}[\text{B}(\text{OR})_4]$ in a straightforward reaction as shown in figure 4.²

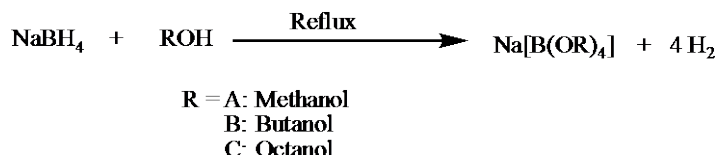


Figure 4 - The synthesis of sodium tetraalkoxyborate.

Due to the fact sodium borohydride was used the reaction was kept under inert (Ar) atmosphere at all times and the product was stored in the glove box. The reaction is entropically favoured as a result of the formation of hydrogen gas, giving yields no lower than 90% of the sodium salt $\text{Na}[\text{B}(\text{OR})_4]$. The next stage of this work is to react the alkoxyborate anion with trimethylsilyl cyanide (TMSCN) to form sodium alkoxytricyanoborates for the form $\text{Na}[\text{B}(\text{OR})(\text{CN})_3]$. These have been reported to yield free-flowing ionic liquids. In this work, a range of different alcohols are under investigation to identify if and how does the carbon chain affect the functionality of the resultant ionic liquid, generating some fundamental structure-property relationship rules that will guide further work. The proposed synthesis of the ionic liquid is shown in figure 5.³ TMSCN is moisture and air sensitive releasing hydrogen cyanide upon contact with air/moisture, which means the reaction will also be carried out under inert atmosphere.

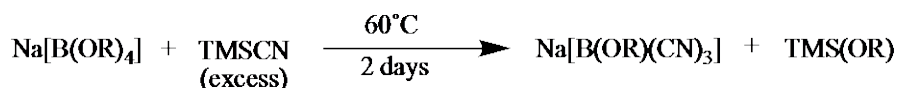


Figure 5 - Proposed reaction scheme for the synthesis of alkoxytricyanoborates.

References:

1. C. Chiappe, F. Signori, G. Valentini, L. Marchetti, C. Pomelli and F. Bellina, *J. Phys. Chem. B*, 2010, **114**, 5082-5088.
2. Campaña, A., Fuentes, N., Gómez-Bengoa, E., Mateo, C., Oltra, J., Echavarren, A. and Cuerva, J., *Org. Chem.* 2007, **72**, 21, 8127–8130.
3. Schopper, N., Sprenger, J., Zapf, L., Reiss, G., Ignat'ev, N. and Finze, M., *New J. Chem.*, 2021.

QUILL Quarterly Report

November 2020 – January 2021

Name:	Marian Borucki		
Supervisor(s):	Prof Peter Nockemann, Dr Stephen Glover & Dr Małgorzata Swadźba-Kwaśny		
Position:	PGR Student		
Start date:	01.2018	Anticipated end date:	07.2021
Funding body:	Bryden Centre, Horiba Mira		

Lithium ion Batteries Degradation Study Using Spectroscopy Techniques

Background

Lithium ion batteries (LIB) are a secondary (rechargeable) battery that are currently the main energy storage device. LIBs are applied in various applications as in portable devices, grid energy storage, grid current regulation as well as in hybrid- and electric vehicles. Energy harvested by the renewable energies is often environmental dependent, what results in discontinuous energy supply. In order to store energy that have been over generated during less energy consuming times of a day, energy storage stations based on LIB are used. The other, yet not less important, application is one where LIBs are replacing the fossil fuel by storing the energy for transport sector, namely in hybrid (HEV) and electric vehicles (EV). The trend of replacing the fossil fuels both in energy sector by supplementing them with renewable energy power plants as well as by supporting the market of HEV, EV and fuel-cell vehicles (FCEV) is growing. New policies of EV30@30 and New Policy Scenario are the programmes that are aimed in expanding the market of HEV, EV and FCEV, thus the supply for lithium ion batteries will grow. Yet, for the market to growth the research, ones that solve current issues, are needed. Automotive council UK in their roadmap report for the lithium ion batteries have gathered up the issues that are needed to be addressed if the automotive of EV, HEV and FCEV is to grow. Such an issues are based on the need of improving the safety of battery usage, lowering the costs of the batteries, researching a new materials for the batteries that will allow to store more energy and provide more power, thus be fast chargeable, issues concerning the battery pack and modules combination, one that will allow to minimize the losses related to cell joining, as well as their thermal management, increasing the lifespan of the batteries as well as increase their recyclability, eventually the research on the next gen batteries is needed.

In order to meet all the requirements a thrill study of the current batteries as well as the development of a new chemistries is needed. Lifespan as well as the safety of the battery is nowadays ones of the most important factor when it comes to the battery application in the transportation market. Battery life is limited by the degradation mechanism, ones that occur inside the cell. Currently there are known number of such mechanism occurring, even though the proper investigating technique allowing *in operando* study have not been developed yet. Moreover, the degradation is highly chemistry dependent so whenever the new chemistry is tested for the battery the new degradation mechanism could occur. On the other hand, the safety of the battery is limited by the usage of the organic based electrolyte, which is highly flammable and might lead to battery explosion. Proper electrolyte, non-toxic, environmentally friendly, non-flammable as well as of high performance should be developed. With developing the new electrolyte, often the development of the electrodes is needed as the electrolyte stability as well as the energy density of the battery highly depends on them.

Objective of this work

The aim of the PhD programme is focused on investigating the lithium ion battery (LIB) degradation processes occurring inside the cell during its operation. In order to achieve the goal a development of an experimental method based on the spectroscopy analysis techniques will be needed. A proper method would allow to observe and measure the changes that occur *in operando* inside the lithium ion battery. During the PhD programme an analytical data of LIB degradation will be acquired, using various analytical techniques including electrode surface examination, electrolyte composition. Acquired spectroscopy data will be linked with the rest of the data gathered in order to develop the sensing method. Eventually, batteries of a different cell chemistries will be investigated.

Working from home summary

During the period of the lockdown the previously assembled lithium ion battery samples have been aged and monitored throughout the period using battery analyser remotely. The impedance data of aged lithium ion cells obtained in pre-lockdown period have been analysed by applying the distribution of a relaxation times (DRT) analysis. Firstly, due to the fact that DRT is able to estimate only resistive and capacitive-resistive behaviour of studied system a pre-processing of impedance data was undertaken. The pre-processing has been investigated and an approach that yield most reliable data has been chosen. Additionally, an investigation of DRT analysis itself has been performed. The DRT analysis could be performed either using the piecewise linear approach or by the use of radial basis function (RBF) for discretization of an EIS data, thus both approaches have been studied. The DRT has been undertaken by the use of DRTtools MatLab® toolbox using MatLab® software. Additionally, knowing that the DRT analysis is heavily dependent on the parameters used that are not commonly discussed, especially for specific electrochemical systems an investigation of optimal value of regularization λ and RBF shape factor μ parameters as well as the regularization derivative has been investigated. The investigation has resulted in obtaining the most optimal set of regularization parameters. As the optimal parameters have been found a DRT analysis has been performed for the impedance data of aged cells.

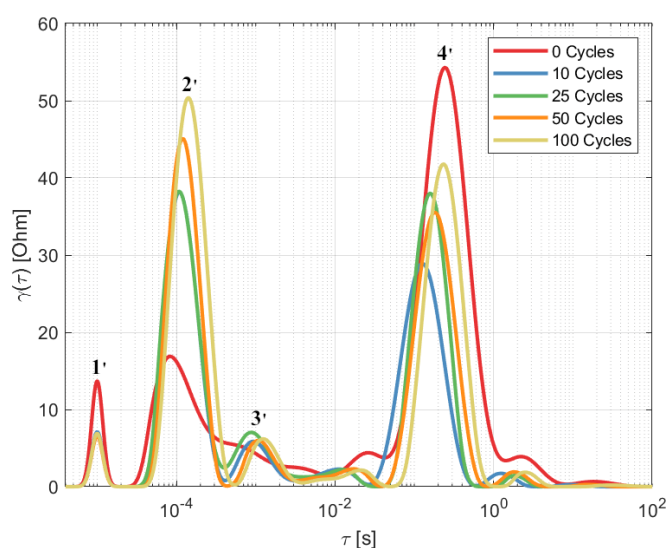


Figure 1 - Distribution of relaxation times analysis of impedance data acquired from CR2032 lithium ion battery of graphite-NMC811 electrode and 1 M LiPF₆ in EC:EMC (1:1 mol) electrolyte performed at state of life equal to 0, 10, 25, 50 and 100 cycles.

It has been observed that the peaks 2' - 4' are characterized by the increasing time constant, yet only peak 2' is characterized by constant polarization resistance increase. The polarization resistance of peak 4' although increased from 10 cycle to 100 cycle point of life it is not observed to be increasing

constantly between the impedance measurements. The polarization resistance for peak 3' is not observed to be changed significantly as the battery is aged although the time constant is observed to be age dependent. As peaks 2' and 4' are characterized by the highest area under peak in relation to other observed peaks, their contribution to the overall polarization resistance is significant to the point that change in their characteristics influence the overall lithium ion battery performance.

The interpretation of observed peaks has been undertaken based on literature. The peak 1', that is characterized by lowest time constant $\tau = 10^{-5}$ / highest frequency of $f = 100 \text{ kHz}$ has been interpreted to be a response of a particle/particle resistance within electrode or the current collector/electrode material interface resistance. The interpretation could be further confirmed by the fact that the electrochemical processes do not occur at frequencies of that magnitude. Additionally, the observed peak is independent on the battery age indicating that no change in electrode/current collector contact interface occurred. The peak 3' could be interpreted as a SEI layer response as given response is observed at τ between 10^{-3} to 10^{-2} , which is the region where SEI layer response is predicted to be observed.

However, in order to confirm the interpretation of the peak nature the state of charge dependency studies should be further undertaken. Peak 4' of τ between 0.13 – 0.23 s could be interpreted as originated from the charge transfer process according to literature. The temperature dependency studies would be an invaluable in confirming the interpretation. Overall, the increase of total polarization resistance throughout the battery ageing has been observed, which have been due to the polarization resistance increase observed for peaks 2' and 4'.

Back to laboratory work tasks

Electrochemical studies – The Lithium ion cells has been studied by impedance spectroscopy at set State-of-Charge levels. The analysis of data by distribution of relaxation times is undertaken. Eventually, the SoC – peak dependency would allow to assign the observed peak to an electrochemical process. The methodology of temperature based studies has been drafted; samples are in preparation.

Post-mortem studies – The *post-mortem* case has been designed, 3D printed and tested for laser beam permittivity using Witech alpha 300R microscope with a control sample as for leakage proving to be sealed. The aged samples are planned to be dismantled in a glovebox. The electrodes are to be sliced in half using ceramic knife into two parts. A four samples, two for cathode and two for anode, are expected to be obtained per sample. The as prepared *post-mortem* samples are to be used for spectroscopy data collection as well as for structural microscopy studies and crystallographic studies. The obtained data from *post-mortem* studies would provide insights to the specific degradation processes occurring inside the cell as the cell is aged and could be further compared to electrochemical data obtain during sample ageing.

Semi-solid electrolyte 'Ionogel' studies – Mechanical properties investigation in cooperation with school of aerospace and mechanical engineering in planning as interschool laboratory access is limited. Synthesis optimization – establishing the substrates molar ratio which result in product of highest ionic conductivity as well as the most optimal mechanical characteristics. Lithium transference number for electrolytes of each substrate ratio is needed to be studied.

Carbon-based anodes spectroscopic ageing comparison – Three carbon-based materials are studied as an anode for the lithium ion cells. A similarity in their ageing mechanism is expected to be

investigated. A broad spectroscopy studies is in order to provide insights if the ageing of different carbonaceous materials is able to be observed by obtaining their spectra in the same conditions.

In operando studies – The methodology for cutting electrodes to shape has been investigated resulting in foil metal cutters to provide with the finest cuts suitable for electrode reshaping. The *in operando* casing, stamp that would allow for design shape cut and sample holder have been developed using SOLIDWORKS® software and has been printed on Ultimaker® 3D printer. Due to delays in delivery the studies were needed to be postponed for mid-March.

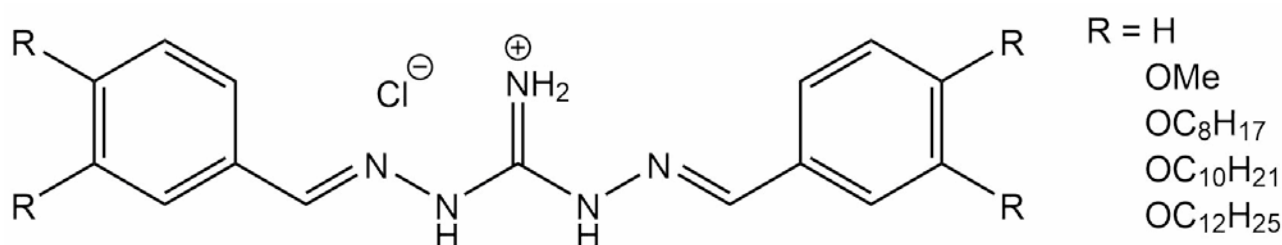
QUILL Quarterly Report

November 2020 – January 2021

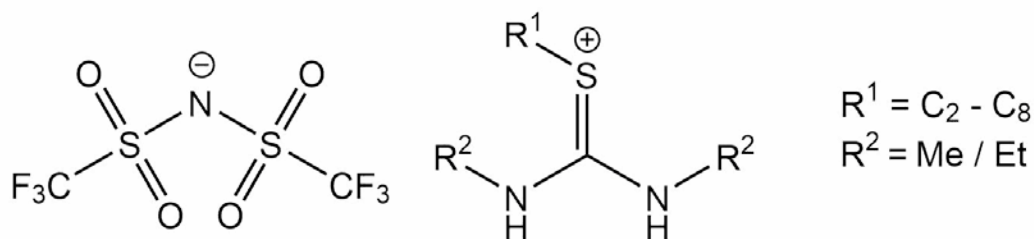
Name:	Dominic Burns		
Supervisor(s):	Prof John Holbrey and Dr Gosia Swadzba-Kwasny		
Position:	PhD Student		
Start date:	1 st October 2019	Anticipated end date:	31 st May 2023
Funding body:	EPSRC		

Recycle and Reuse of Process Water Through Sulfate Removal: Developing an Ionic Liquid Technology for Selective Anion Recognition and Extraction

The previous quarter has focussed on the synthesis of proposed micelle forming sulfate extractants (shown below) based on the monofunctional di(imino)guanidinium complex reported by Bruce Moyer *et al* (DOI: 10.1039/c8cc05115a). These compounds require a two or three step synthesis with the last step being an alkylimino-de-oxo-bisubstitution reaction with the corresponding 3,4-dialkoxybenzaldehyde and 1,3-diaminoguanidine hydrochloride. While apparently simple, the synthesis has proven challenging and the methodology to prepare these materials has had to be reevaluated. New experimental conditions to prepare model unalkylated, methoxy and decyloxy analogues have been successfully identified and progress is on-track to generate materials for investigation of their structure-activity relationship in terms of self-assembly and sulfate extraction ability.



Within QUILL, Holbrey *et al* previously studied IIs with thiuronium cations in 2009 (DOI: 10.1039/c0nj00098a). The potential to generate thiuronium-sulfate ion pairs through hydrogen-bonding molecular recognition are underway, to establish whether this cation type, in a hydrophobic form, is a good lead for further investigation. Early studies involving short chain thiuronium cations were inconclusive as there was a significant amount of leaching of the IL into the aqueous phase, this prevents quantification of aqueous sulfate concentration by X-ray fluorescence analysis due to interference from sulfur in the cations.



QUILL Quarterly Report

August 2020 – October 2020

Name:	Andrew Forde		
Supervisor(s):	Dr Stephen Glover, Dr Rob Watson & Prof Peter Nockemann		
Position:	PhD Student		
Start date:	03/06/2019	Anticipated end date:	03/12/22
Funding body:	Horiba-MIRA & EPSRC		

Battery Thermal Management and Algorithmic 3D Temperature Prediction

Experimental

One aim of this project is to place thermal sensors close to the active materials in a prismatic cell for model validation purposes. In order to carry this out, an instrumentation process has been designed and tested on a 3D printed model of the cell. This testing highlighted the requirement for precision in placing sensors as piercing of the jelly roll within the cell would cause damage to the cell and possibly lead to the occurrence of thermal runaway. For this reason, additional equipment has been designed to add further precision to sensor placement. This is currently being tested using the 3D printed cell to prove that sufficient accuracy and repeatability can be achieved before moving on to the instrumentation of a real cell.

Machine Learning

Machine learning has been used in this project with the aim of producing an accurate and computationally efficient method for temperature prediction. Previously, this was carried out using an LSTM (Long-Short Term Memory) network in order to produce a time-series prediction of internal battery temperature in 1D. This has since been expanded to use a Bidirectional LSTM in order to attain more accurate predictions and faster training times. This method was then used to predict the voltage response of a battery and the same 1D internal temperature, shown in Figures 1 and 2.

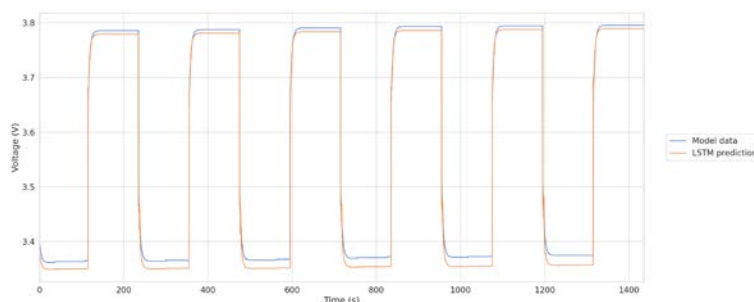


Figure 1 - Voltage prediction using numerical model vs. bidirectional LSTM

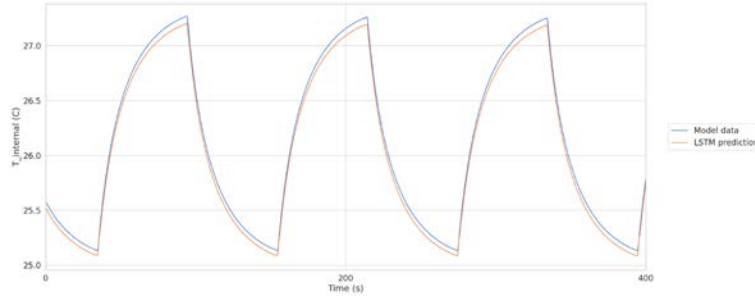


Figure 2 - Internal temperature prediction using numerical model vs. bidirectional LSTM

This same prediction method was then used to carry out a 3D prediction of temperature throughout the battery. Figure 3 shows the results of the numerical model used for training the network, along with the prediction made by the neural network and the error between the two. These results show that error increases in areas of low uniformity and that error compounds over time. This is due to the network using its previous prediction to inform its prediction for the next time step, therefore error accumulates as the predictions continue to be made.

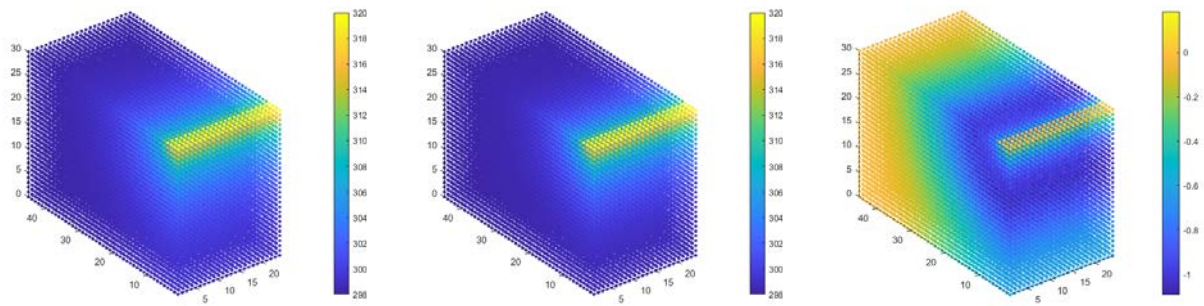


Figure 3 - Bidirectional LSTM prediction of temperature within half of a prismatic cell 30s after initial condition (All colourbar measurements in Kelvin). From left to right: (a) Prediction from FEA numerical model, (b) Prediction from Bidirectional LSTM network, (c) Error between numerical model and LSTM prediction

One method for solving this issue is the use of physics informed neural networks. These operate similarly to other neural networks, however, can introduce governing equations in predictions. This allows for the inclusion of conservational laws and known theory in the neural network. Use of these methods for this project are currently being investigated.

QUILL Quarterly Report

November 2020 – January 2021

Name:	Oisin Hamill		
Supervisor(s):	Nancy Artioli (1) Alex Goguet (2)		
Position:	PhD Student		
Start date:	01/10/2019	Anticipated end date:	30/09/2022
Funding body:	EPSRC		

Mechanism Understanding of NO_x Storage, Release and Reduction on Pt/doped Ceria Catalysts

Background

Due to strengthening emission legislations in Europe, North America and the rest of the world, there is a need for further optimisation of existing emission after-treatment catalytic converters for automotive applications. New legislations focus primarily of NO_x abatement and consequently the exhaust emissions of lean-burn gasoline and diesel vehicles. After treatments systems must utilise new technologies to reduce this that offer low temperature activation and high stability.

High surface area ceria is successfully employed as an excellent support of metals (Pd, Rh, Pt, etc.) in commercial catalytic systems for the oxidations of carbon monoxide and propane and automotive emission control. Ceria is a unique material with a rich and complex chemistry. It possesses high oxygen storage capacity (OSC), a unique redox property by the cycle of Ce⁴⁺/Ce³⁺ redox pairs and it can be further enhanced through using dopants. Platinum supported on ceria can show enhanced NO_x storage at low temperature, as reported in the literature, together with an improved carbon monoxide/hydrocarbon light off.

Ceria supported catalysts, in general, do not operate efficiently at low temperatures and therefore must be modified in order to overcome this problem. For this reason, addition of enhancing materials is currently being considered in detail. This addition of a material that increases the performance of an already functional catalyst is called doping. The main function of this dopant is to allow the catalyst to function outside of the normal working temperature range and operating conditions to increase catalyst efficiency.

It has been proposed that the dopants, such as rare-earth and transition metal oxides, increase the concentration of surface vacancies which affect the ionic conductivity, oxygen mobility and oxygen storage capacity of the ceria. It can be speculated that all these properties are responsible for the enhanced oxidation activity by promoting oxygen diffusion and formation of more "reactive oxygen" species. Furthermore, the oxygen species play a role in the mechanism of the reaction, favouring the NO_x storage.

Additionally, presence of dopants can reportedly modify the platinum reducibility and platinum-ceria interaction, allowing more readily activation during rich purge.

This project aims to better understand the NO_x storage mechanism on the doped materials and give new insights into the activation/lean deactivation mechanisms in the presence of different dopants.

Objective of this work

The main objective considered in this project is to improve the understanding of the NO_x storage mechanism, together with the mechanism of rich purge on ceria supported platinum. We aim to gain a deeper knowledge of the rich activation and lean deactivation mechanisms as well as determine the structure of the active sites under reaction conditions. We look to develop a method to differentiate between active species and spectator species through transient methods. We will also strive to develop a global kinetic model for the reaction and all involved species. This will enable the determination of the relative importance of different reactions within the catalyst bed as well as a measurement of the exact gas compositional conditions present during the reactions. With this approach in depth information relevant to mechanistic understanding and reaction engineering application will be obtained.

Progress to date

- Addition of water CEM to rig in order to create a more consistent and stable water flow rate in feed lines – did not work. Reverted to original glass bulb saturator.
- TPR characterisation completed for all catalysts.
- BET characterisation completed for most catalysts.
- Addition of Ar purge gas line to feed into rig just before reactor.
- Addition of bypass valve and line in rig to immediately re-route all feed gas from mass spec line to bypass line.
- Lean/Rich cyclic experiments started.
- TPD Ar purge temperature measured and stated to be around 450C and 10 minute hold.

Conclusions and future work

- Effect of doping evident.
- Next steps involve completing LEAN/RICH cycling experiments.
- Complete NSC tests at 200, 300 and 450C on high pt loaded ceria catalysts.

QUILL Quarterly Report

November 2020 – January 2021

Name:	Jerry Pui Ho Li		
Supervisor(s):	Dr Nancy Artioli & Prof Peter Nockemann		
Position:	Research Fellow		
Start date:	9/12/2020	Anticipated end date:	8/02/2021
Funding body:	Invest Northern Ireland		

A Catalytic Gas-to-Liquid Process for CO Valorisation

The project being contracted for is titled: A Catalytic Gas-to-Liquid Process for CO Valorisation. This is largely work with more emphasis towards commercialisation and business, with some towards academic goals (when possible).

Objective of this work

This is work based around the commercialisation of a catalytic process, requiring first to identify the market area and reaction. This is followed by a work plan (WP) broken down into several stages:

1. Identifying the type of catalyst required followed by optimising the catalyst.
2. Designing a lab scale multi-channel reactor using the optimised catalyst in WP1.
3. Perform a techno-economic analysis of a scaled-up process, using the work from WP1 and 2 as the core basis.

The project also requires more business-oriented tasks, making industrial contacts, partners, and mentors through and outside of tradeshow and conferences.

Other work beyond the project itself involve the technical support for the research group itself, whether it be laboratory maintenance or to provide aid to the students.

Progress to date

During this period, more focus has been placed on the experimental work of the proof of concept (POC) project. At present we are able to satisfy the goals of CO₂ conversion, upwards of 25%. The product distribution produced requires further optimisation however.

On the commercial end of the work, engagement has been made with Aggregate (also known as LaFarge) concrete manufacturing. They are keen on any carbon conversions technology as one of the bigger CO₂ emitters globally, and have shown interest in discussions. This had resulted in an introductory meeting with representatives of Aggregate, with all those involved in the POC in attendance. It would appear that there has been interest, with parties on both sides drawing up NDA agreements before further discussion. Within the meeting, an introduction to our proposed technology was made, showing conversion of CO₂ to hydrocarbons. Preliminary results were presented, introducing the type of catalyst to be used, and some reaction data. Aggregate meanwhile, have highlighted their need for carbon emission control but also highlighted the purity of their flue gas. It would appear that in addition to the conversion, the flue gas requires some cleaning and purification.

In the benchmark samples, each sample based from XRD analysis indicate successful formation of the desired Fe_3O_4 , with an average particle size within 10 nm. However, in comparison to the literature data, the conversions while comparable (max of CO_2 conversion of 25% for our results, ~30% in the literature), selectivity is not as literature produces a higher selectivity of higher chain hydrocarbons. For our samples we observe mainly C1-C6. Thus the ionic liquid set can only be compared with our own benchmark results.

In the ionic liquid set, it was found that the benchmark method of introducing Na promoter cannot be done in the ionic liquid template, as it was found that the NaOH precipitating agent reacts with the ionic liquid, forming NaF on the surface as indicated through XRD analysis, and based on experimental reaction results showed that it had completely poisoned the catalyst making it completely inactive. Thus Na promoters need to be added to the catalyst post-synthesis, thus not a completely fair test compared to the benchmark samples.

The reaction results indicated that for the benchmark samples, C2-C4 and C5+ hydrocarbon selectivity increases with higher Na content. As indicated previously however, the selectivity amount does not match that of the literature. In each instance, methane selectivity remains high, ranging 60-90%. Thus suggests that while CO_2 conversion is happening, there is still a higher preference to methanation and not active enough to allow for oligomerization to form the hydrocarbons.

The reaction results for the ionic liquid set of samples show results with comparable conversions at low Na content, but becomes has reduced conversion with higher Na content. The hydrocarbon selectivity is slightly less than that of the benchmark samples but similarly maintains higher methane selectivity. The use of the ionic liquid chosen does not appear to have improved on hydrocarbon selectivity. In addition, its application may add additional difficulties as it is much more necessary to completely wash the newly synthesized Fe_3O_4 followed by post synthesis adding of Na promotor. It is also important to note that it is unlikely the ionic liquid can be recycled due to it being miscible in water, HCl, and the NH_4OH precipitating agent (in place of NaOH). Thus this process using the materials on hand is only feasible if CO_2 conversion was higher and with much higher hydrocarbon selectivity.

For the technoeconomic analysis, the figures for our best reaction results were used between CO_2 and H_2 . Due to Aggregate not returning after the initial meeting, an accurate composition of the flue gas from the concrete manufacturing process was not given. Thus in all the simulations, flue gas from an AD plant process was used. While not the same, it provides an optimistic projection using an impure gas stream that requires the CO_2 to be cleaned. The economic analysis conducted shows that at present, the running of this plant is not feasible. Based on the simulation from our current results, the process would have a capital cost of 2.8M USD, with a total operating cost of 1.6M USD/yr. Based on the market price of LNPG (50 USD/MT, value taken from McKinsey & Company). Based on the gas composition produced, we have produced Heavy LNPG which produces less energy than natural gas but is relatively cleaner. Based on the market price and simulated scale, this would produce ~33k USD/year of profit. This is already lower than the current operating costs. In addition, LNPG production is sensitive to seasonal changes due to the difference in boiling temperatures of C3 and C4 components. Although the overall cost of CO_2 scrubbing is relatively low (145.4 USD/tonne), the H_2 expense is high (4950 USD/tonne). Thus if keeping with the current CO_2/H_2 ratio, increasing the process flow will increase the product formed in the end, but also process costs. Thus with just the products formed at present, the process costs exceed that of the profits generated. One possible way to offset this is through H_2 recovery and storage though H_2

value is also relatively low but with high market demand (16.51 USD/MT). The analysis is only partially optimized however, due to the short amount of time in the overall project duration.

In other general tasks, one of the FTIR spectrometers was recovered with the goal of future usage.

QUILL Quarterly Report

November 2020 – January 2021

Name:	Sam McCalmont		
Supervisor(s):	Dr Leila Moura, Prof John Holbrey & Prof Margarida Costa Gomes		
Position:	PhD		
Start date:	Jan 2020	Anticipated end date:	2023
Funding body:	EPSRC Doctoral Training Partnership		

Chemisorbent Materials for Olefin and Paraffin Separation

Develop and test new chemisorbent materials for the separation of light olefins and paraffins. In this, achieving high capacity and selectivity for the selected materials. To test this, equipment will be installed, commissioned, and benchmarked for testing under approximate industrial gas stream compositions.

Progress to date:

The main objective since the last quarterly report is the continued commissioning of the gas system. The volume (V_x) determination of the chambers (equilibrium and mixing) and pipework is required for the pressure-volume-temperature (pVT) measurements. The simplified version of these chambers and pipework can be seen in Figure 1. V_1 is the mixing chamber, V_2 is the connecting pipework between chambers and V_3 is the equilibrium chamber. The gas system also allows for headspace gas chromatography (HSGC) and with high pressure nuclear magnetic resonance (HP NMR) analysis to be utilised. The HSGC allowing for composition of the gas to be known in the pVT measurements when multiple gases are introduced. The NMR to see how the gas interacts with the chemisorbent materials. The pVT measurements will be used to determine the solubility of different gases in different chemisorbent materials. Carbon dioxide solubility in polyethylene glycol 200 (PEG200) will be the first solubility determined on the gas system as part of the benchmarking phase.

The phosphorus based ionic liquids trihexyltetradecylphosphonium diisooctylphosphinate ($[P_{666(14)}][DiOP]$) and 1-butylimidazolium dimethylphosphate ($[C_4C_1Im][DMP]$) are being characterised for a joint project with Prof Margarida Costa Gomes. This involved the synthesis and characterisation of ($[C_4C_1Im][DMP]$), and the characterisation of a previous batch of $[P_{666(14)}][DiOP]$. The characterisation includes NMR, CHNS, TGA, DSC, water content and mass spectrometry analysis. Over the last month, initial runs have been conducted with the HP NMR with ethylene and ethane in $[P_{666(14)}][DiOP]$.

The data collected from the solubility calculations will be compared against the industrial standard of cryogenic distillation. This will be completed with ASPEN plus. This will involve creating a database of ionic liquid and then different chemisorbent material on ASPEN plus to be able to compare against cryogenic distillation.

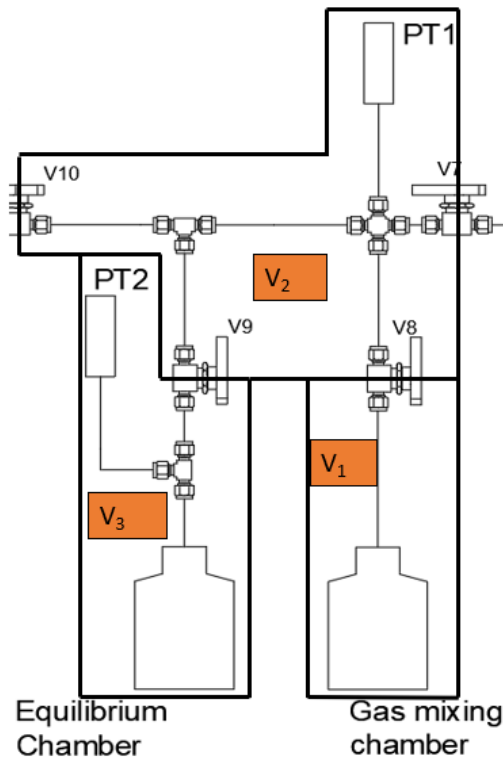


Figure 1 - The three volumes (V_x) of the gas system required for the pVT measurements: V_1 the gas mixing chamber, V_2 the connection between the chambers and location of one of the pressure transmitters (PT) and V_3 represents the equilibrium chamber and the second pressure transmitter. The VX notation represent valves.

QUILL Quarterly Report

November 2020 – January 2021

Name:	Anne McGrogan		
Supervisor(s):	Dr Gosia Swadzba-Kwasny		
Position:	PhD		
Start date:	01/10/2019	Anticipated end date:	31/03/2023
Funding body:	EPSRC		

Boron Lewis Acids: Structure and Applications

Transition metals are widely recognised for their ability to function as good catalysts, but they have major drawbacks such as low abundance, high cost and toxicity. Boron is a main group, non-metallic, earth-abundant element with the potential to replace transition metals.¹ Many boron-based species show very strong Lewis acidity (*i.e.* excellent electron-pair acceptors).² However, understanding, quantifying and predicting Lewis acidity is very challenging, which limits the development of boron-based catalysts. Usually, measurement of Lewis acidity is probe-dependent, therefore order of strength on Lewis acidity scale may vary, depending on the probe used and the methodology adopted. In addition, there are limited experimental measurements of electronic structure of boron compounds. A major challenge for obtaining experimental electronic structure data is the presence of the boron centre. The boron 1s core orbital has an energy of ~200 eV, meaning that vacuum conditions are required for any electronic structure measurements. I am currently working on a study which will utilise liquid-microjet x-ray spectroscopy using the soft x-ray synchrotron BESSY II, Berlin, to determine the valence electronic structure of boron-containing samples. This research will be done in collaboration with Dr Kevin Lovelock from the University of Reading, who will be analysing the results. The aim is to use this data to better quantify, understand and predict the Lewis acidity of boron-based species. By understanding how the electronic structure relates to chemical reactivity, it will help aid the design of new boron based catalytic systems. To achieve this goal a combination of liquid-jet sample delivery with x-ray photoelectron spectroscopy (XPS), resonant XPS (RXPS) and x-ray absorption spectroscopy (XAS) will be used to study a range of boron-containing samples. These include reference samples and a selection of 3 and 4 coordinate boron-based species with formal charges -1, 0, +1. Suggested samples are shown in Table 1.

Boron 1s XPS, along with calculations, will be used to probe the atomic charge of the boron centres; this is important for understanding and predicting reactivity. The atomic charge for ligands bonded to boron will also be probed (O 1s, Cl 2p, P 2p).

RXPS is a site-specific technique involving resonant core level excitation followed by de-excitation through Auger electron emission. The boron-based molecular orbitals (MO) for all compounds are expected to be at a similar binding energy to solvent MOs. Using standard XPS, identification of boron-based solute MOs would be very difficult due to how they are swamped by signal from solvent MOs. RXPS of B 1s will allow identification of these boron-based MOs. Furthermore, RXPS will allow identification of MOs from ligands bonded to boron (O 1s, Cl 2p, P 2p).

B 1s XAS will be recorded using partial Auger yield detection (as part of the RXPS measurements). XAS, along with time-dependent DFT calculations, will be used to identify the boron-based unoccupied MOs. In addition, unoccupied MOs for ligands bonded to boron will be identified (O 1s, Cl 2p, P 2p).

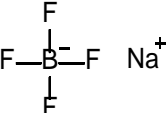
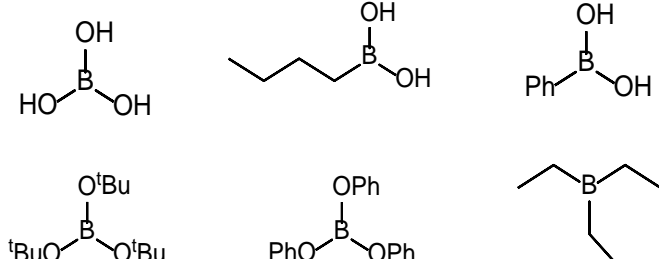
Objective of this work

The aim is to gain a better understanding of how the electronic structure of boron-based species relate to chemical reactivity which will help aid the design of new boron based catalytic systems.

Progress to date

I have been designing the sample set of boron compounds to be tested at BESSY II in May. Table 1 shows some of the compounds that will be tested and then the synthesis of some boron compounds will be described.

Table 1 - Structures of the samples along with the coordination number and formal charge

Molecule/ion	Coordination number	Formal charge
	4	-1
	3	0

The product of the dehydration of phenyl boronic acid with 2-aminobenzyl alcohol is shown in Figure 1. This tricoordinate neutral compound was obtained in quantitative yield in a Dean-Stark reactive distillation using toluene as mass agent.

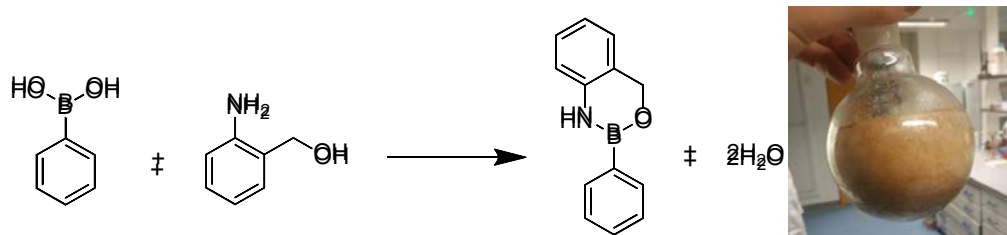


Figure 1 - Dehydration of phenyl boronic acid with 2-aminobenzyl alcohol

A Bronsted acid could also be added (Figure 2) to generate the borenium cation. Resonance equilibria show the decentralisation of the positive charge.

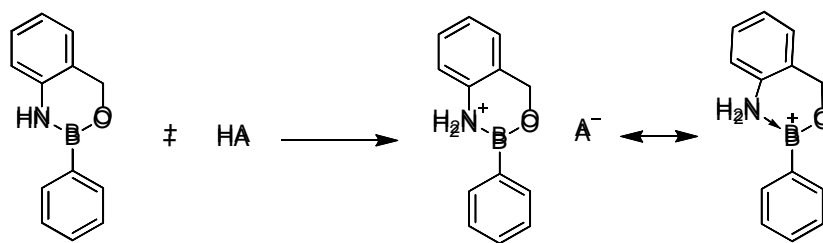


Figure 2 - Protonation of tricoordinate boron compound to generate borenium ionic liquid.

The product of dehydration of phenyl boronic acid with pinacol was also synthesised using dean-stark apparatus. The product, shown in Figure 3 was a low viscosity liquid. Developing this further, a number of small molecule boric acid esters and boronic acid esters were generated (Figure 4), each being low viscosity liquids.

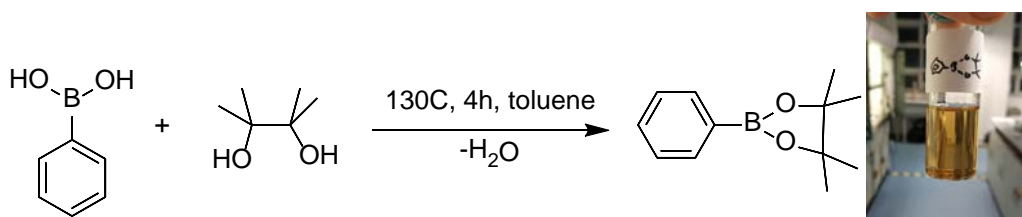


Figure 3 - Dehydration of boric phenyl boronic acid with pinacol

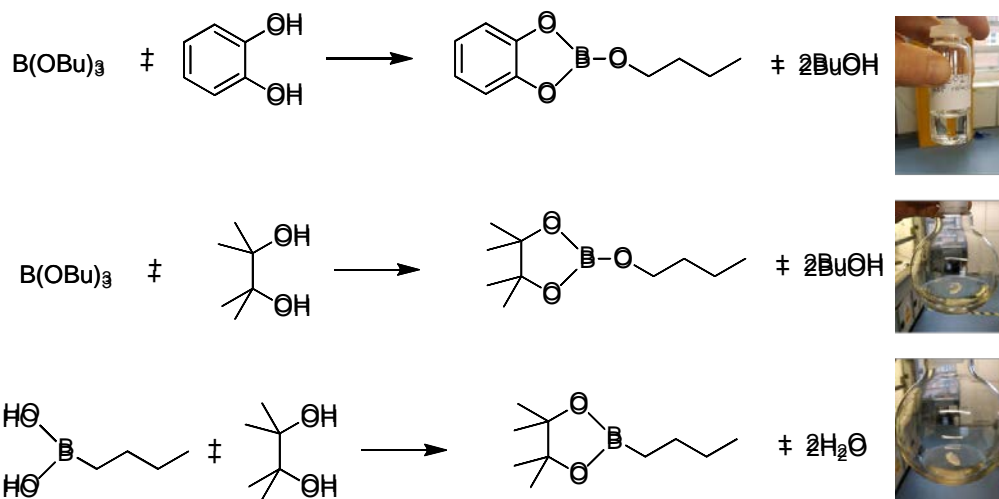


Figure 4 - Reaction of tributyl borate with catechol and pinacol as well as dehydration of butyl boronic acid with pinacol

These compounds were made by adding 1 equivalent of the starting materials and heating to reflux in toluene, followed by distillation of butanol or collection of water in dean-stark apparatus. The compounds will be fully characterised using NMR, mass spec, DSC and TGA. The sample set has been designed to enable

comparisons to be made between boron compounds of different coordination numbers and different charges. L-donors such as trioctylphosphine oxide (TOPO) can also be added to these tricoordinate compounds to investigate tetracoordinate boron species (Figure 5).

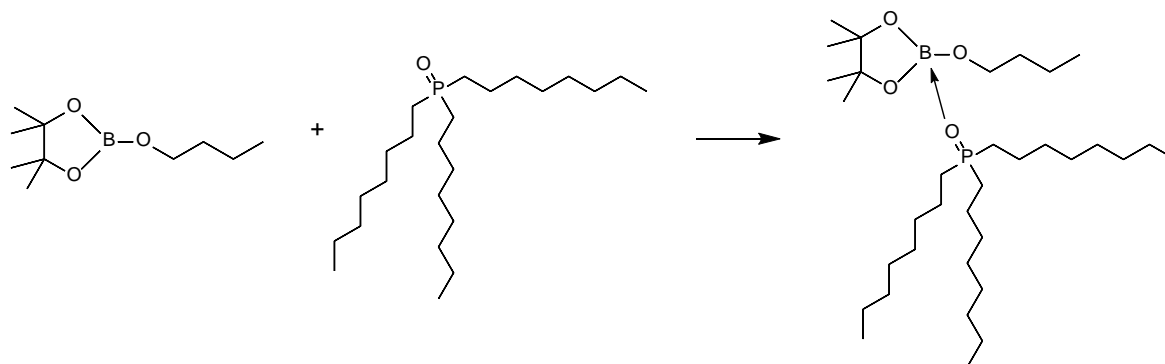


Figure 5 - Reaction of butyl boronic acid ester with trioctylphosphine oxide.

Addition of O-donor (TOPO) and N-donors (octylamine and trioctylamine) to Bpin(OBu) resulted in a mixture of both 3 and 4-coordinate compounds. The ^{11}B NMR spectrum (Figure 6) shows the development of a tetracoordinate boron species upon addition of TOPO, with a new broad peak in the spectrum at 3.15 ppm. There is also the presence of a peak in the tricoordinate region which is more deshielded by $\Delta^{11}\text{B} = 11.65$ ppm with respect to Bpin(OBu).

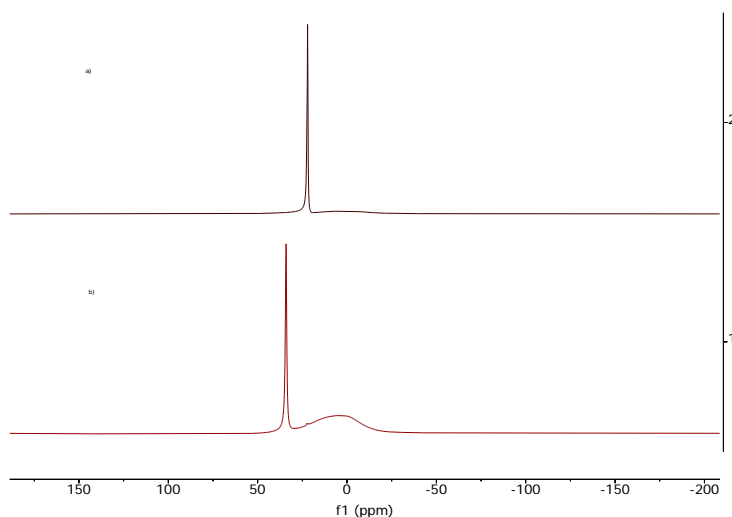


Figure 6 - Comparison of ^{11}B NMR spectra illustrating the change of boron environment from a) Bpin(OBu) on the addition of 1 equivalents of b) TOPO.

I have also been learning how to use EPSR and Dissolve modelling programmes to analyse neutron scattering data. I have been analysing data comparing the liquid structure of: (a) neat sulfuric acid, (b) an ionic liquid made of two moles of sulfuric acid and one mole of pyridine, and (c) a mixture of one mole of sulfuric acid, one mole of pyridine and two moles of water. This work will give an important insight into the liquid structure, explaining some of their unique properties and hopefully enabling further optimisation. Analysis of the results so far, show that this model has responded to the experimental data input by generating an un-ionised, molecular representation of sulfuric acid. Furthermore, the results show that pyridine is protonated. Further analysis into the liquid structure and hydrogen bonded network will be undertaken.

Conclusions and future work

Preparations are in progress to run experiments at BESSY II in May. The sample set is evolving to contain more boron compounds and to ensure that useful comparisons can be made. This work will give an important insight into the electronic structure of these compounds which will help to better quantify their Lewis acidity and to aid the design of new catalytic systems. Future work will involve full characterisation of boron compounds, as well as investigating the addition of TOPO and trioctylamine to the tricoordinate boron compounds synthesised.

References

1. M. A. Legare, C. Pranckevicius and H. Braunschweig, *Chem. Rev.*, 2019, **119**, 8231-8261
2. S. Coffie, J. M. Hogg, L. Cailler, A. Ferrer-Ugalde, R. W. Murphy, J. D. Holbrey, F. Coleman and M. Swadźba-Kwaśny, *Angew. Chem.-Int. Edit.*, 2015, **54**, 14970-14973.

QUILL Quarterly Report

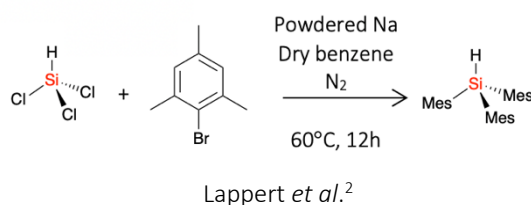
November 2020 – February 2021

Name:	Shannon McLaughlin		
Supervisor(s):	Dr Gosia Swadźba-Kwaśny		
Position:	PhD Student (1 st year)		
Start date:	October 2020	Anticipated end date:	July 2024
Funding body:	Department for the Economy		

Thinking Inside the (Glove)Box: Lewis Superacidic Ionic Liquids Based on Main Group Cations

The main aim of this project is to research main group cations such as tin, aluminium, gallium, indium and silicon as potential components of new Lewis Superacidic ionic liquids. Initial research has focused on cationic silicon compounds and the first goal of this project is to synthesise the ‘free’ trimesitylsilylium cation first isolated by Lambert et al. In order to synthesise this cation methods described by Lappert et al., Zigler et al.³ and Lambert et al. will be followed to synthesise trimesitylsilane, chlorotrimesitylsilane and allyltrimesitylsilane, respectively. Finally, allyltrimesitylsilane will be used to synthesise the ‘free’ trimesitylsilylium cation. The complete synthesis has been illustrated in the previous QUILL quarterly report. Delayed arrival of the trichlorosilane starting reagent for the synthesis of trimesitylsilane (Scheme 1) has prevented any further progress.

Scheme 1 - Synthesis of trimesitylsilane



Side Projects:

Synthesis of imidazolium, phosphonium and perfluorinated ionic liquids.

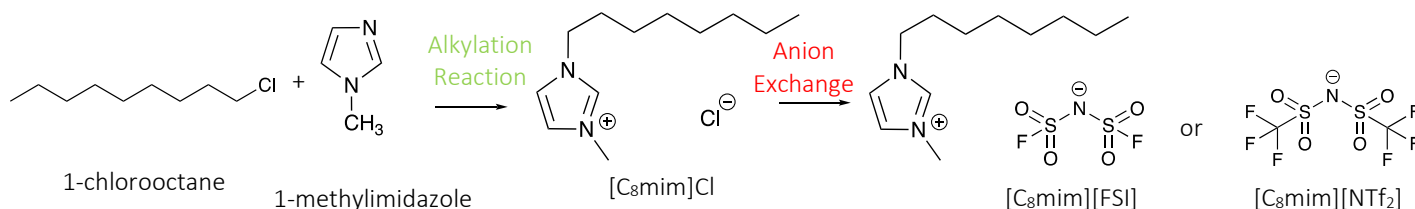
Continuation of previous research into the hydrogenation of organic substrates using frustrated Lewis pairs (FLPs) in ionic liquids.

Synthesis of Ionic Liquids

Synthesis of Imidazolium based Ionic Liquids:

1-octyl-3-methylimidazolium chloride ([C₈mim]Cl) was synthesised *via* an S_N2 alkylation between 1-methylimidazole and 1-chlorooctane. [C₈mim]Cl was then converted to either 1-octyl-3-methylimidazolium bis(trifluoromethylsulfonyl)imide ([C₈mim][NTf₂]) or 1-octyl-3-methylimidazolium bis(fluorosulfonyl)imide ([C₈mim][FSI]) *via* an anion exchange reaction (Scheme 2). 10 ml of [C₈mim][NTf₂] and [C₈mim][FSI] was synthesised and sent away for further research.

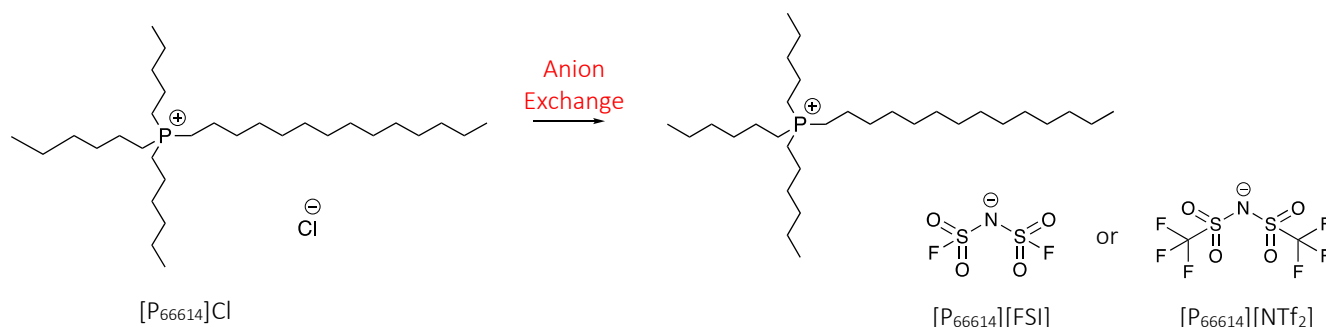
Scheme 2 - Synthesis of [C₈mim][NTf₂] and [C₈mim][FSI]



Synthesis of Phosphonium based Ionic Liquids:

Trihexyl(tetradecyl)phosphonium chloride [P₆₆₆₁₄]Cl was converted to either trihexyltetradecyl-phosphonium bis(trifluoromethylsulfonyl)imide ([P₆₆₆₁₄][NTf₂]) or trihexyltetradecyl-phosphonium bis(fluorosulfonyl)imide ([P₆₆₆₁₄][FSI]) *via* an anion exchange reaction (Scheme 3). 10 ml of [P₆₆₆₁₄][NTf₂] and [P₆₆₆₁₄][FSI] was synthesised and sent away for further research.

Scheme 3 - Synthesis of [P₆₆₆₁₄][NTf₂] and [P₆₆₆₁₄][FSI]

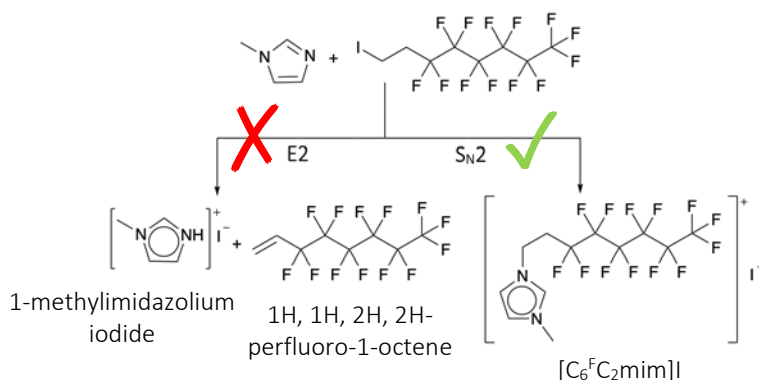


Synthesis of Perfluorinated Ionic Liquids:

1-methyl-3-(1H, 1H, 2H, 2H-perfluorooctyl)imidazolium iodide ([C₆^FC₂mim]I) was synthesised *via* an S_N2 alkylation between 1-methylimidazole and 1H, 1H, 2H, 2H-perfluoro-1-iodooctane. [C₆^FC₂mim]I was then converted to either 1-methyl-3-(1H, 1H, 2H, 2H-perfluorooctyl)imidazolium bis(trifluoromethylsulfonyl)imide ([C₆^FC₂mim][NTf₂]) or 1-methyl-3-(1H, 1H, 2H, 2H-perfluorooctyl)imidazolium bis(fluorosulfonyl)imide ([C₆^FC₂mim][FSI]) *via* an anion exchange reaction. Reactions were monitored using ¹H, ¹³C and ¹⁹F NMR spectroscopy. 10 ml of [C₆^FC₂mim][NTf₂] and [C₆^FC₂mim][FSI] will be synthesised and sent away for further research.

One of the main synthetic challenges in this reaction is the competition between the desired S_N2 alkylation and an E2 reaction illustrated in Scheme 4. The E2 reaction produces 1-methylimidazolium iodide and 1H, 1H, 2H, 2H-perfluoro-1-octene as by products. XRFs of the final ionic liquids showed that there was still iodine present as an impurity. It has proved extremely difficult to remove this impurity even after washing the ionic liquids multiple times.

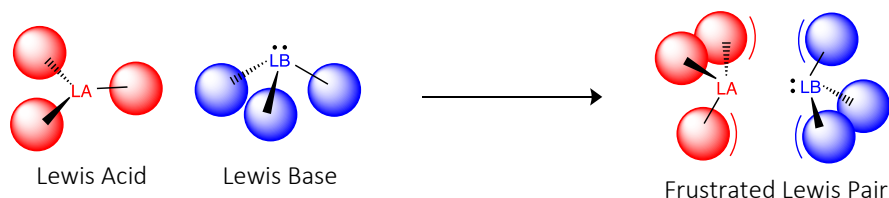
Scheme 4 - Competing synthetic routes



Hydrogenation of Organic Substrates using Frustrated Lewis Pairs in Ionic Liquids:

Frustrated Lewis pairs (FLPs) are compounds or mixtures containing a Lewis acid and a Lewis base that cannot combine to form a classical adduct due to steric hindrance (Scheme 5). The close proximity of these free Lewis acidic and Lewis basic sites gives rise to interesting reactivity. FLP chemistry has helped to develop catalysts for metal-free reduction of organic unsaturated substrates and CO₂. It has also been used as a strategy to allow main group compounds to activate small molecules, including metal-free hydrogen splitting.

Scheme 5 - Formation of a sterically hindered FLP between a Lewis acid and a Lewis base.



Preparation of Frustrated Lewis Pair (FLP) Solutions in Ionic Liquids/*d*₆-benzene:

The FLP made from tri-*tert*-butylphosphine (P(*t*Bu)₃) and tris(pentafluorophenyl)borane (B(C₆F₅)₃) has previously been studied by both Stephan *and the Swadźba-Kwaśny group*. It been shown to effectively split hydrogen in both *d*₆-benzene and in [C₁₀mim][NTf₂]. In both cases uptake of hydrogen by the FLP system was confirmed by the formation of a new pair of broad peaks of approximately equal integration in the ¹H NMR spectra. This demonstrated the ability of the FLP system to split hydrogen in the ionic liquid medium, despite the very low solubility of molecular hydrogen in ionic liquids.

Expanding on this research, 160 mmol solutions of four different FLPs have been made up in *d*₆-benzene, [C₂mim][NTf₂] and [C₁₀mim][NTf₂] (Figure 1). The four different phosphorus compounds investigated were tri-*tert*-butylphosphine, trioctylphosphine, tri-1-naphthylphosphine and diphenyl(pentafluorophenyl)phosphine (Figure 2). These phosphorus compounds were chosen as they are all sterically hindered either with branched groups, long alkyl chains or rings attached. This makes them attractive targets to potentially form FLPs when combined with B(C₆F₅)₃. Solutions were prepared in a glovebox and the progress of reaction was monitored using ¹H, ¹³C, ³¹P, ¹⁹F and ¹¹B NMR spectroscopy. All three solutions made with tri-1-naphthylphosphine were white and cloudy as neither the P(1-naphthyl)₃ or B(C₆F₅)₃ completely dissolved at this concentration.

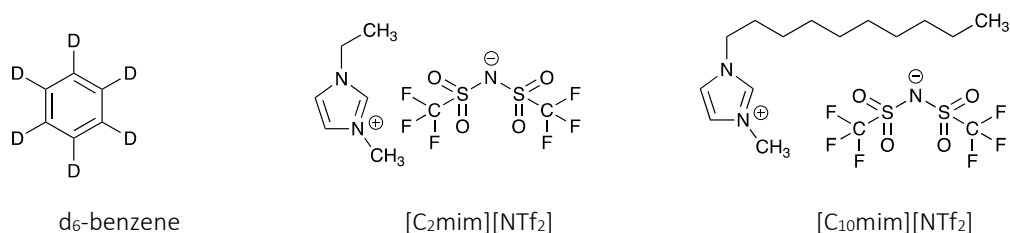


Figure 1 - Structure of solvents under investigation

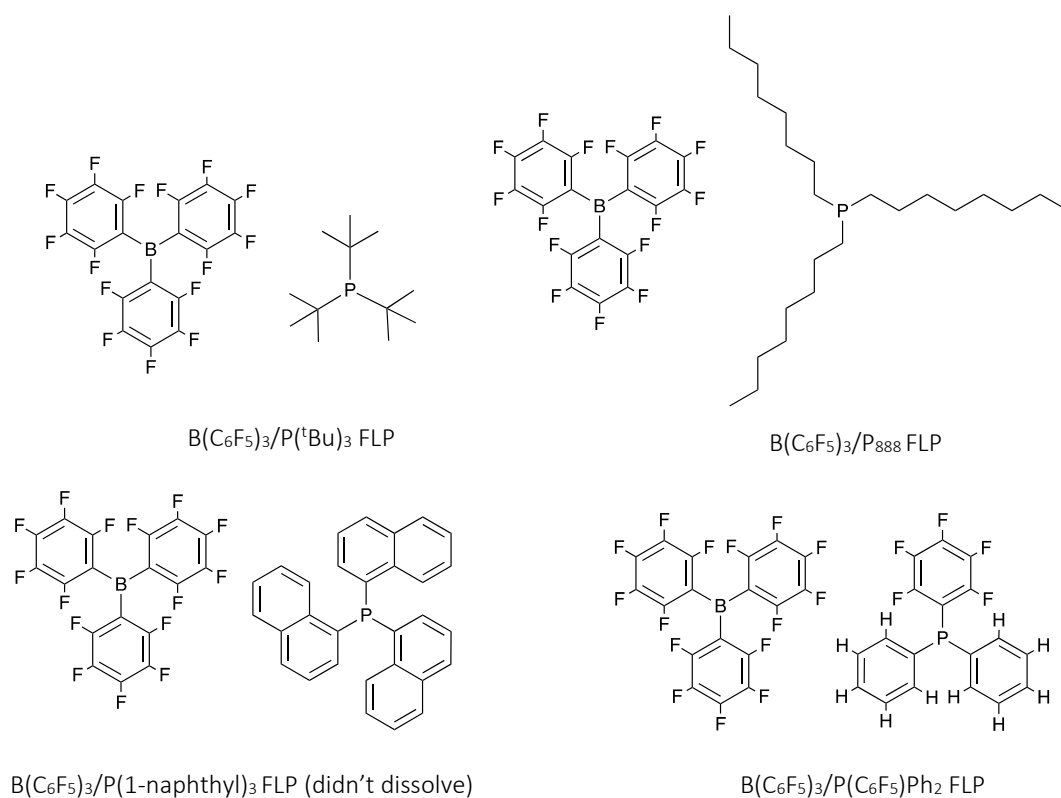


Figure 2 - Structure of FLPs under investigation

Hydrogenation of Organic Substrates:

Pure hydrogen gas will be bubbled through the FLP solutions for 12 hours. A novel NMR tube illustrated in Figure 3 was designed with a wider neck allowing a septum to be attached and two needles connected. This setup allows H_2 to be bubbled through the FLP in d_6 -benzene/ionic liquid directly in the NMR tube. This unique design will hopefully improve contact between the hydrogen and the ionic liquid as well as encouraging gas transfer.

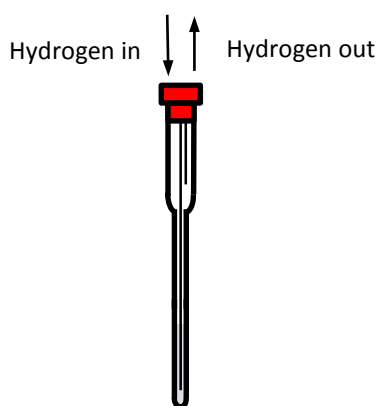
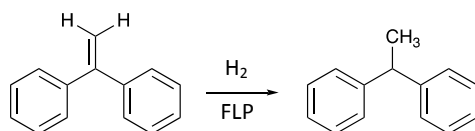


Figure 3 - Diagram of hydrogenation setup

The reduction of 1,1-diphenylethylene will then be investigated (Scheme 6). These organic substrates have been chosen as they have been previously observed in literature to be effectively reduced by FLP systems.

Scheme 6 - Reduction of 1,1-diphenylethylene to 1,1-diphenylethane.



References:

1. J. Lambert et al. Crystallographic evidence for a free silylium ion. *Science* 297, 825–827 (2002).
2. M. Gynane, M. Lappert, P. Riley, P. Rivière and M. Rivière-Baudet, *Journal of Organometallic Chemistry*, 1980, 202, 5-12.
3. S. Zigler, L. Johnson and R. West, *Journal of Organometallic Chemistry*, 1988, 341, 187-198.
4. J. Lambert, C. Stern, Y. Zhao, W. Tse, C. Shaul, K. Lentz and L. Kania, *Journal of Organometallic Chemistry*, 1998, 568, 21-31.
5. J. M. Breen, S. Olejarz and K. R. Seddon, *ACS Sustain. Chem. Eng.*
6. D. W. Stephan, *J. Am. Chem. Soc.*, 2015.
7. D. W. Stephan and G. Erker, *Angew. Chemie - Int. Ed.*, 2015, 54, 6400–6441.
8. D. W. Stephan, *Acc. Chem. Res.*, 2015, 48, 306–316.
9. J. Lam, K. M. Szkop, E. Mosaferi and D. W. Stephan, *Chem. Soc. Rev.*, 2019.
10. M. A. Courtemanche, M. A. Légaré, L. Maron and F. G. Fontaine, *J. Am. Chem. Soc.*, 2014, 136, 10708–10717.
11. G. C. Welch, R. R. San Juan, J. D. Masuda and D. W. Stephan, *Science* (80-.), 2006, 314, 1124–1126.
12. G. C. Welch and D. W. Stephan, *J. Am. Chem. Soc.*, 2007, 129, 1880–1881.
13. L. C. Brown, J. M. Hogg, M. Gilmore, L. Moura, S. Imberti, S. Gärtner, H. Q. N. Gunaratne, R. J. O'Donnell, N. Artioli, J. D. Holbrey and M. Swadźba-Kwaśny, *Chem. Commun.*, 2018, 54, 8689–8692.
14. L. Greb, P. Oña-Burgos, B. Schirmer, S. Grimme, D. W. Stephan and J. Paradies, *Angew. Chemie – Int. Ed.*
15. S. Tamke, C.G. Daniliuc and J. Paradies, *Org. Biomol. Chem.*

QUILL Quarterly Report

November 2020 – January 2021

Name:	Hugh O'Connor		
Supervisor(s):	Prof P Nockemann and Dr S Glover		
Position:	PhD Student		
Start date:	October 2019	Anticipated end date:	June 2023
Funding body:	EPSRC		

Redox Flow Battery Design

Designs for 3D-printed Redox Flow Battery cells have been finalised and are currently being evaluated in the battery lab at QUILL. The cells have been subjected to a rigorous set of tests, consisting of long charge/ discharge cycles, polarization tests and EIS. Each test is being carried out at different flow rates and electrode compressions do demonstrate the robustness of the cell design. These results show favourable comparisons to those found in literature and will also be compared to a commercially available cell. This experimental work is being carried out on a bespoke test rig which has been designed and manufactured in house during the past number of months. The polymers used to produce the 3D-printed cells (PP and ABS) are also being tested for chemical compatibility with a number of commonly used flow battery supporting electrolytes. In parallel with this work, development of a coupled CFD/ electrochemical model has continued and has been used in the design process for these 3D-printed cells.

QUILL Quarterly Report

November 2020 – January 2021

Name:	Zara Shiels		
Supervisor(s):	Dr Artioli, Prof Nockemann & Dr Harrison		
Position:	PhD		
Start date:	Feb 2019	Anticipated end date:	2022
Funding body:	Interreg (Renewable Engine Project)		

Developing New Nanocatalysts for the Direct Conversion of Biogenic Carbon Dioxide (CO₂) to Sustainable Fuels

Initial testing of previous samples deemed to have too many inconsistencies to provide useable data. It was decided that due to different issues with the gas rig itself that these should be fully investigated and rectified before continuing with testing. It was discovered that due to blockages occurring in the back pressure regulator (a cold spot was able to occur) where the hydrocarbons being formed in the reaction were able to build up over a number of runs finally resulting in a complete blockage of the system. This was rectified by installing a much longer heating tape, improving the heating of the back pressure regulator itself by reconfiguring the way in which the heating tape was utilised and installing more thermocouples to determine the heating across multiple points of the line. Through the new thermocouples it was discovered that the temperature previously used was not sufficient and so an increased temperature has since been able to be established. Another cold spot was determined to be in the vent line of the system allowing gas to vent before reaching the GC in order to avoid build of pressure, where hydrocarbons had been able to condense out, which has also had a new heat tape installed in order to avoid this issue in the future. Due to these improvements in the system, we have been able to effectively test 4 different samples and improve the amount of condensate collected after the reaction for further analysis.

The table below provides a summary of the samples that have been tested to date.

Synthesis Method	Conditions	Support Used	Method of Combination	Sample Name
Precipitation	With Na	HZSM-5 (80)	Granular mixing	PM-WithNa-HZSM-5(80)-GM
Precipitation	With Na	HZSM-5 (80)	Ball Milling	PM-WithNa-HZSM-5(80)-BM
Precipitation	With Na	HZSM-5 (300)	Granular mixing	PM-WithNa-HZSM-5(300)-GM
Precipitation	With Na	ZIF-67	Granular mixing	PM-WithNa-ZIF-67-GM
Precipitation	With Na	Aluminium Terephthalate	Granular mixing	PM-WithNa-AlTerephthalate-GM

At this time the data is still being elaborated to determine the CO₂ conversion and the selectivity to the different products formed.

QUILL Quarterly Report

Nov 2020 – Jan 2021

Name:	Yaoguang Song		
Supervisor(s):	Prof Peter Nockemann & Prof David Rooney (QUB), Dr Xiaolei Zhang (Strathclyde), Prof Stuart Gibb & Dr Szabolcs Pap (UHI)		
Position:	PGR Student		
Start date:	3 rd Dec 2018	Anticipated end date:	31 Dec 2021
Funding body:	EU INTERREG VA Programme, managed by SEUPB		

Thermochemical Conversion of Biomass Lignin into Mesoporous Carbon Materials

Background

As a main component, lignin from biomass holds huge potential for producing mesoporous carbons (MCs), which represents upper-class valuable products amongst all lignin-based applications. However, most preparation methods for MCs are empirical, leading to unpredictable topologic and structural properties thus likely unfavourable for aimed downstream applications. Soft-templating synthesis was reported successful to tune nanostructures effectively, but novel promising templates are still in need of development.

Considering that ionic liquids (ILs) are increasingly seen in the dissolution and depolymerisation of lignin and certain ILs with long alkyl chain on the cations exhibit excellent amphiphilic properties, thus are potential structure-directing agents. This programme aims to investigate the possibility to convert lignin into MCs by employing ILs. The effective implementation involves both experimental work and computational investigation via molecular dynamics (MD) simulations.

My last quarterly report introduced the coarse-grained (CG) MD simulations to investigate how the third chemical species influence the assembly process of ILs in water. Phenolic compounds, namely phenol, resorcinol, and phloroglucinol, were selected as a vague model of lignin to study the feasibility of employing amphiphilic ILs as template. From CG-MD simulations, we noticed that the increasing hydroxyl groups of phenolic compounds influence both the morphologies of ILs and the distribution of phenolic compounds themselves. My recent work mainly focused on the experimental work to verify the simulation results.

Results

1) Synthesis of [C₁₀MIM][OAc]

1-alkyl-3-methylimidazolium-based ILs are the most studied family so far. Herein, 1-decyl-3-methylimidazolium acetate ([C₁₀MIM][OAc]) was chosen as potential template.

[C₁₀MIM][OAc] was prepared via a typical two-step method: the alkylation of 1-methylimidazole with 1-bromodecane and metathesis reaction for anion exchange from bromide to acetate. The products were characterised by NMR spectroscopy to ensure no detectable impurity. ¹H and ¹³C NMR spectra were recorded on Bruker Avance III 400 MHz NMR spectrometer.

1-methylimidazole (0.40 mol, 99%, Sigma-Aldrich) was mixed in toluene (400 mL, ≥99.7%, Sigma-Aldrich) with slightly excess of 1-bromodecane (0.44 mol, 98%, Sigma-Aldrich). The flask was placed to stir at 110 °C oil bath under reflux for 24 h. Toluene was carefully removed by rotavapor then the

product was further washed with diethyl ether (200 mL, $\geq 99.5\%$, Sigma-Aldrich) for 3 times. $[C_{10}MIM][Br]$ was obtained as yellowish viscous oil (yield: 88%). 1H NMR (chloroform-d, 400 MHz): δ 10.11 (s, 1 H), 7.58 (s, 1 H), 7.38 (s, 1 H), 4.15 (t, 2 H), 3.96 (s, 3 H), 1.73 (m, 2 H), 1.00-1.20 (m, 14 H), 0.68 (t, 3 H). ^{13}C NMR (chloroform-d, 100 MHz): δ 137.0, 123.8, 122.1, 50.0, 36.6, 31.7, 30.2, 29.3, 29.2, 29.1, 28.8, 26.1, 22.5, 13.9.

For the metathesis reaction, $[C_{10}MIM][Br]$ was firstly dissolved in absolute ethanol ($\geq 99.8\%$, Fisher Scientific) with KOAc ($\geq 99\%$, Sigma-Aldrich), then above mixture was stirred at ambient temperature for at least 2 h. Slight excess of KOAc was necessary to guarantee the displacement of Br^- . White precipitate was filtered to separate the insoluble KBr out of solution, where the latter was evaporated by rotavapor to remove ethanol. Cold acetone ($\geq 99.8\%$, Fisher Scientific) was then added and the flask was left in refrigerator for 12 h to totally precipitate KBr and excessive KOAc. After filtering again, potassium salts were totally removed then remainder acetone was evaporated by rotavapor. The product was further purified under ultra-high vacuum system at 50 °C overnight. $[C_{10}MIM][OAc]$ was finally obtained as yellowish oil, less viscous than $[C_{10}MIM][Br]$ (yield: 94%). 1H NMR (chloroform-d, 400 MHz): δ 10.80 (s, 1 H), 7.39 (s, 1 H), 7.35 (s, 1 H), 4.06 (t, 2 H), 3.87 (s, 3 H), 1.72 (m, 2 H), 1.72 (m, 3 H), 0.80-1.30 (m, 14 H), 0.64 (t, 3 H). ^{13}C NMR (chloroform-d, 100 MHz): δ 177.1, 139.2, 123.2, 121.5, 49.6, 35.9, 31.5, 30.1, 29.1, 29.0, 28.9, 28.7, 26.0, 25.4, 22.4, 13.9.

2) Preparation of IL/water/phenolic compounds ternary mixtures

Phenolic compounds were purchase from Sigma-Aldrich and used as received. Molar ratio of three chemical components are according to CG-MD simulations as shown in Table 1.

Mixtures	$\frac{IL}{IL+water}$ wt%	Phenolics	Morphologies from simulation	
ILs + water + phenolics			298.15 K	358.15 K
1000 + 140000 + 1000	10.07%	phenol	spherical	spherical
2000 + 125400 + 2000	20.00%	phenol	spherical	spherical
3000 + 72000 + 3000	39.51%	phenol	spherical	spherical
3000 + 48000 + 3000	49.49%	phenol	spherical	spherical
3250 + 40000 + 3250	56.02%	phenol	hexagonal columnar	spherical
3500 + 36000 + 3500	60.38%	phenol	hexagonal columnar	hexagonal columnar
4000 + 32000 + 4000	66.21%	phenol	hexagonal columnar	hexagonal columnar
4300 + 28000 + 4300	70.65%	phenol	hexagonal columnar	lamellar bilayer
4600 + 24000 + 4600	75.03%	phenol	lamellar bilayer	lamellar bilayer
4600 + 16000 + 4600	81.84%	phenol	lamellar bilayer	lamellar bilayer
3250 + 40000 + 3250	56.02%	resorcinol	spherical	spherical
4000 + 32000 + 4000	66.21%	resorcinol	spherical	spherical
4600 + 24000 + 4600	75.03%	resorcinol	hexagonal columnar	hexagonal columnar
4600 + 16000 + 4600	81.84%	resorcinol	hexagonal columnar	hexagonal columnar
4600 + 24000 + 4600	75.03%	phloroglucinol		
4600 + 16000 + 4600	81.84%	phloroglucinol	hexagonal columnar	hexagonal columnar
3000 + 48000 + 3000	49.49%	benzene		
4600 + 16000 + 4600	81.84%	benzene	lamellar bilayer	lamellar bilayer

Table 1 - Summary of ternary systems with final morphologies from CGMD simulations

3) Small-angle X-ray Scattering (SAXS):

SAXS measurements were planned to carry out for above three-component systems to probe the morphologies, as well as binary mixtures for comparison. Generally, the ratio of scattering vector q peak values $q_1:q_2:q_3:q_4=1:\sqrt{3}:\sqrt{4}:\sqrt{7}$ indicates a characteristic hexagonal periodicity, while ratio $q_1:q_2:q_3 = 1:2:3$ corresponds to smectic lamellar phase.

However, available SAXS facilities are in Great Britain. Owing to the pandemic with ensuing lockdown nationwide, unfortunately the delivery and characterisation are delayed significantly. The tests would be performed until the cease of lockdown.

4) Polarised Optical Microscopy (POM)

Phase examinations were performed under an Olympus BX50 microscope at 298.15 K. All samples textures were determined after heating firstly to beyond clear point wherever possible then cooling down to 298.15 K with a Linkam TH600 hot stage and TP 92 temperature controller.

However, no LLCs or lyotropic gels were observed at 298.15 K under optical microscope for $[C_{10}MIM][OAc]/\text{water}/\text{phenol}$ ternary mixtures with hexagonal columnar and smectic lamellar morphologies, which generally appear in lyotropic IL/water mixtures. Fig. 1a) shows the lyotropic texture of $[C_{10}MIM][OAc]/\text{water}$ mixture at IL content of 82 wt%, while it is clear isotropic phase in ternary mixture at same IL content (Fig. 1b). Undoubtedly this phenomenon is associated with the introduction of phenol that destabilised the periodic three-dimensional H-bonding lattices between ILs and water hence the disappear of liquid crystalline mesophase. Especially the hydroxyl group of phenol is good H-bond functionality, both H-bond donor and acceptor, due to the conjugation between one of the two lone electron pairs of O atom and electrons on aromatic ring forming a large π bond, which favours the interaction with ILs and water. In the neat long-chain 1-alkyl-3-methylimidazolium salts, the crystalline phase exhibits highly ordered lamellar array at lower temperature and changes into an enantiomeric smectic phase or directly form isotropic liquids after melting. Analogous temperature dependent phase transitions were reported in IL/water binary mixtures as well. Apparently, alongside of heating to break H-bonds, the introduction of a new component into a IL/water binary system also plays an important role in disarranging cation structure by participating H-bonding interactions. Even liquid crystalline phase disappeared in a ternary system, the strong H-bonding ability of anion like acetate still effectively stabilised the array of cations into various morphology.

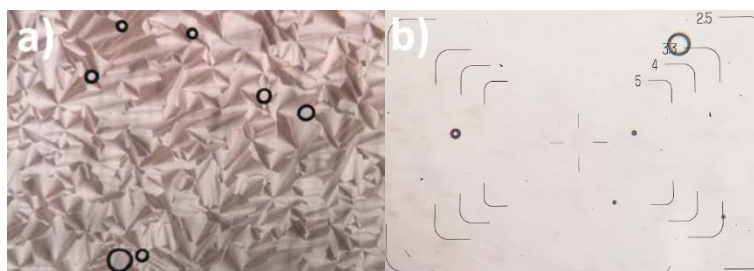


Figure 1 - POM images of lyotropic phase: a) $[C_{10}MIM][OAc]/\text{water}$ binary mixture; b) $[C_{10}MIM][OAc]/\text{water}/\text{phenol}$ ternary mixture

Similar with IL/water/phenol mixtures, no lyotropic gels or LLCs was found for ternary systems with resorcinol or phloroglucinol added when hexagonal columnar and lamellar morphologies appeared. While such phenomenon didn't apply to IL/water/benzene cases, where texture of lyotropic gel was visible under optical microscope as shown in Fig 2a. Indeed, liquid crystalline phase were also observable in $[C_{16}MIM][Br]/\text{water}/p\text{-xylene}$ ternary mixture. This is because both benzene and *p*-xylene have no functionalities that are composed of atoms with lone electron pairs like oxygen and nitrogen thus are able to function as H-bond donor or acceptor. Consequently, benzene and *p*-xylene are chemically stable in mixture and won't destroy the periodicity of H-bonding lattice between IL and water. However, when the molar ratio of IL to phenolic compound was reduced less than 1, lyotropic gels were observed for ternary mixtures containing phenolic compounds (Fig 2b). This phenomenon provides another evidence that phenolic compounds disordered the H-bonding network between ILs and water. Therefore, when ILs outnumber phenolic compounds the excessive

ILs could maintain periodic H-bonding lattice with water and showed lyotropic gels from macroscopic aspect.

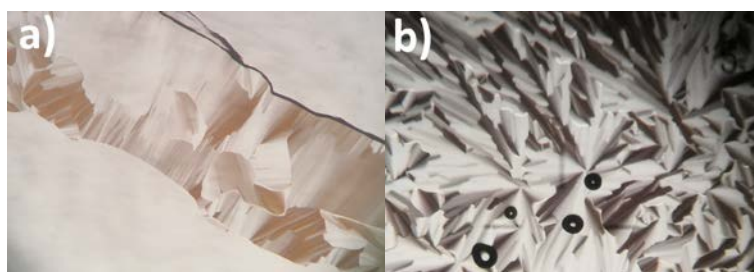


Figure 2 - POM images of lyotropic phase: a) [C10MIM][OAc]/water/benzene ternary mixture at the ratio of 1:3.48:1; b) [C10MIM][OAc]/water/resorcinol ternary mixture at the ratio of 1:3.48:0.5

Although researchers tend to associate different texture patterns to certain lyotropic phases, the identification of ordered hexagonal columnar and smectic lamellar phase by performing optical microscopy alone is quite challenging and could lead to ambiguous even deceptive results without the combination of other characterisation techniques since some typical texture patterns are observable in both lyotropic mesophases. Especially in this work, the lyotropic crystals/gels may unlikely form when involving a third chemical specie (i.e. phenolic compounds) but IL cations still displayed in an well-ordered way. Thus, the validation of morphologies still requires SAXS measurements for above three-component systems.

5) Preparation of MCs

Another potential validation method is directly to prepare MCs based on simulations and characterise the morphology of MCs. Therefore MCs were prepared using phenolic compounds.

For a typical preparation, 40 mmol phloroglucinol was dissolved in 40 mmol ILs, then 40 mmol glyoxal 40 wt% aqueous solution was added. The vial were sealed and placed into 85 °C oil bath. The addition reaction of glyoxal to phloroglucinol and the polycondensation reaction took place in 20 min.

The obtained resin was washed by water then the water was removed by ratovap to recycled ILs. The yield of recycled ILs reached 65%.

The resin was dried at 85 °C convection oven for 24 h, then calcinated in tube furnace under nitrogen gas. The temperature was heated up to 800 °C for 1 h with heating rate of 1 °C/min.

Carbon materials were submitted to measure surface area and pore structures. Based on simulation, the resin and carbon materials are expected to have hexagonal porous structures. Unfortunately the TEM/SEM facilities are unavailable during lockdown.

Conclusions and future work

Owing to the lockdown, much work has been delayed and needs to be done afterwards. Especially the validation of simulation work using SAXS or solid-state NMR to check the morphology of ILs. Besides, DFT calculations are also under performing to optimise the structure to validate the distribution of phenolic compounds and study the detailed interaction. In the future, 2D NOESY NMR will be performed to study the distribution of phenolic compounds. Other characterisation will also be performed to study the carbon materials based on simulation if appropriate.

References

1. D. Montané, V. Torné-Fernández and V. Fierro, *Chem. Eng. J.*, 2005, **106**, 1–12.
2. Y. Song, J. Liu, K. Sun and W. Xu, *RSC Adv.*, 2017, **7**, 48324–48332.
3. J. M. Rosas, R. Berenguer, M. J. Valero-Romero, J. Rodríguez-Mirasol and T. Cordero, *Front. Mater.*, , DOI:10.3389/fmats.2014.00029.
4. A. M. Puziy, O. I. Poddubnaya and O. Sevastyanova, *Top. Curr. Chem.*, 2018.
5. J. Zhang, B. Dong, L. Zheng, N. Li and X. Li, *J. Colloid Interface Sci.*, 2008, **321**, 159–165.
6. A. E. Bradley, C. Hardacre, J. D. Holbrey, S. Johnston, S. E. J. McMath and M. Nieuwenhuysen, *Chem. Mater.*, 2002, **14**, 629–635.
7. N. Goujon, M. Forsyth, L. F. Dumée, G. Bryant and N. Byrne, *Phys. Chem. Chem. Phys.*, 2015, **17**, 23059–23068.
8. T. Inoue, B. Dong and L. Q. Zheng, *J. Colloid Interface Sci.*, 2007, **307**, 578–581.
9. I. Goodchild, L. Collier, S. L. Millar, I. Prokeš, J. C. D. Lord, C. P. Butts, J. Bowers, J. R. P. Webster and R. K. Heenan, *J. Colloid Interface Sci.*, 2007, **307**, 455–468.
10. P. A. Heiney, in *Handbook of Liquid Crystals*, Wiley-VCH Verlag GmbH & Co. KGaA, Weinheim, Germany, 2014, pp. 1–47.

QUILL Quarterly Report

November 2020 – January 2021

Name:	Richard Woodfield		
Supervisor(s):	Stephen Glover, Robert Watson, Peter Nockermann		
Position:	PhD Candidate		
Start date:	06/2019	Anticipated end date:	12/2022
Funding body:	EPSRC		

Modelling the use of Flow Batteries in Transport Applications

Background

Flow batteries have received significant attention in the past years for use in grid storage applications. The decoupling of the relationship between power and energy density offers a very unique way to store energy to suit the user's particular needs. The extremely long cycle life of a flow-battery is another attractive asset, as the electrodes do not undergo cyclic stressing in the same way Li-ion and other chemistries do. Flow-batteries have received very limited attention regarding their use in transport applications. There is untapped potential in the fact that the discharged electrolyte of a flow-battery could be rapidly swapped at a traditional gas-station, where the infrastructure is already half in-place with storage tanks under the stations. With the electrolyte being entirely re-usable, the station would use an on-site flow-battery to recharge their reservoir and provide passing vehicles with opportunity to swap their electrolyte with readily charged fluid.

Objective of this work

The overall goal of the project is to identify viable electric or hybrid modes of transport that would benefit from the use of a flow-battery, given the refillable nature of the flow-battery electrolyte reservoirs. Even the applications rendered not viable will have outcomes, as the amount by which the energy density of the electrolyte would need to improve by is also providing electrolyte chemists with targets to aim for. The investigations will be carried out using software to model battery and vehicle behaviour, primarily Simulink.

Progress to date

Battery testing was due to start before the pandemic, and the focus has shifted towards the modelling side of the project for the time being. Flow-battery models have been developed, including an electrical and thermal model of a vanadium redox flow-battery coastal ferry, which shows promise.

Conclusions and future work

Battery testing will commence soon, allowing some initial models to be further validated. Hybrid vehicle models will be developed further too.

QUILL Quarterly Report

November 2020 – January 2021

Name:	Mark (John) Young		
Supervisor(s):	Dr Leila Moura, Prof John Holbrey and Prof Sophie Fourmentin		
Position:	PhD student		
Start date:	01-08-20	Anticipated end date:	2024
Funding body:	EPSRC		

Gas Separation Technologies

This project centres around carbon dioxide/methane gas separation which is the major separation in biogas upgrading. We seek to carry out this separation using deep eutectic solvents (DES) whose gas separation properties (capacity and/or selectivity) could be amplified through the use of macrocyclic molecules such as cyclodextrins(CD) and cucurbiturils(CB). These are similar molecules, in terms of both host guest properties and shape, that have been previously reported to have carbon dioxide/methane separation capabilities. Our goal is the superposition of the properties of the DES with that of the macrocycles to form environmentally benign gas upgrading systems.

HS-GC (headspace gas chromatography) sampling and methodology for materials screening has been the major focus of my work this quarter. We will use HS-GC with permanent gasses (carbon dioxide and methane) which will be injected into the HS-GC vials. We will then screen materials for selectivity between the two gasses and possibly for early assessment of gas solubility.

We need to generate calibration curves of peak area against amount of injected gas in order to carry out screening. As of yet no correlation has been found between the pressure of the injected gas and the GC peak area. We have several theories as to what is causing this issue. The first is the gases leaking from the vials. We hope to fix this by testing multiple septa of different makes and materials. Another possible issue is the needle size for gas injection in the vials. We have purchased smaller needles to minimise the puncture wound in the septa to attempt to rule this issue out. The third reason we may not be experiencing linearity is the nature of the GC sampling method as is outlined in Figure 1. During the sample loop filling stage it's possible that venting could be allowing gas to escape and giving lower than expected peak areas. We may be able to mitigate this factor by using carrier gas to add further pressure to the vials and regain a linearity between gas in the vial and peak area. Another option will be to conduct a calibration curve at low pressures only.

Upon completion of the calibration curves for both carbon dioxide and methane we will continue with method development. This will begin with using known materials.

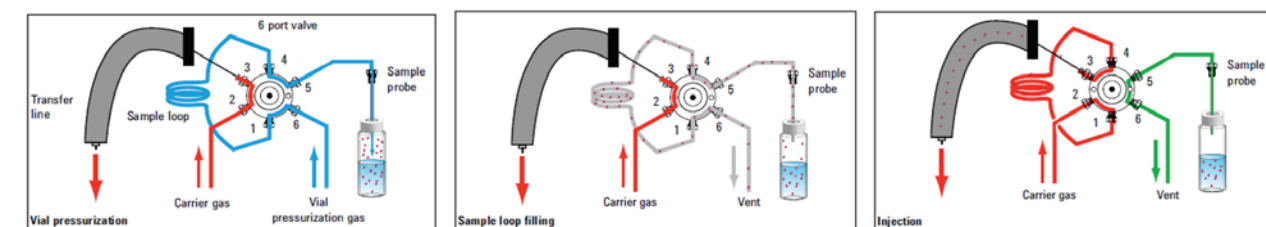


Figure 1 - Headspace GC pressurisation, loop filling and injection diagram

The first material for investigation using HS-GC will be [BMIM][NTf₂] (fig. 2.) which was synthesised according to literature methodology. [BMIM][NTf₂] is known to have a high solubility and selectivity for carbon dioxide and therefore we can use it as a confirmation of HS-GC methodology.

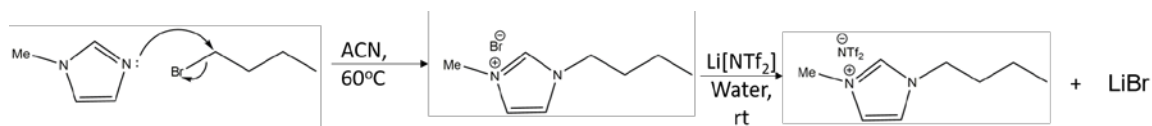


Figure 2 - [BMIM][NTf₂] synthesis and reaction mechanism

We will also use deep eutectic solvents (DES) for confirmation of HS-GC methodology. We will use choline chloride:Urea 1:2 (fig. 3) as it has previously been tested for solubility of both carbon dioxide and methane along with the selectivity between the two gasses.

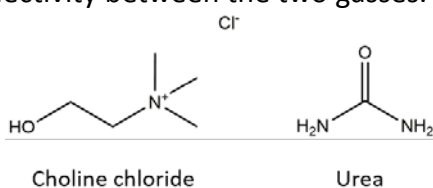


Figure 3 - Structure of choline chloride and urea

We will test these materials with mixed gasses to try to estimate a selectivity for carbon dioxide over methane using HS-GC. These results should align with that of literature values to make our screening process viable to test many systems simultaneously. Any materials which show promise would then be selected to undergo to full PVT measurements.